Biochimica et Biophysica Acta 1850 (2015) 742–749

Contents lists available at ScienceDirect

Biochimica et Biophysica Acta

journal homepage: www.elsevier.com/locate/bbagen

Evolution of the active site of human glutathione transferase A2-2 for enhanced activity with dietary isothiocyanates

Wei Zhang [a,c,d], Daniel F.A.R. Dourado [f], Bengt Mannervik [a,b,e,*]

[a] Department of Chemistry-BMC, Uppsala University, SE-75123 Uppsala, Sweden
[b] Department of Neurochemistry, Stockholm University, SE-10691 Stockholm, Sweden
[c] Department of Chemistry, The Skaggs Institute for Chemical Biology, The Scripps Research Institute, 92037 La Jolla, CA, USA
[d] Department Cell of Molecular Biology, The Skaggs Institute for Chemical Biology, The Scripps Research Institute, 92037 La Jolla, CA, USA
[e] Department of Chemical Physiology, The Scripps Research Institute, 92037 La Jolla, CA, USA
[f] Department of Cell & Molecular Biology, Computational & Systems Biology, Uppsala University, Sweden

ARTICLE INFO

Article history:
Received 4 September 2014
Received in revised form 10 December 2014
Accepted 19 December 2014
Available online 24 December 2014

Keywords:
Glutathione transferase
Isothiocyanate
Directed evolution
Enzyme engineering
Detoxication

ABSTRACT

Background: Organic isothiocyanates (ITCs) are produced by plants, in which they are released from glucosinolates by myrosinase. ITCs are generally toxic and serve as a chemical defense against herbivorous insects and against infections by microorganisms. In mammalian tissues subtoxic concentrations of ITCs can provide protective effects against cancer and other diseases partially by induction of glutathione transferases (GSTs) and other detoxication enzymes. Thus, human consumption of edible plants rich in ITCs is presumed to provide health benefits. ITCs react with intracellular glutathione to form dithiocarbamates, catalyzed by GSTs. Formation of glutathione conjugates is central to the biotransformation of ITCs and leads to a route for their excretion. Clearly, the emergence of ITC conjugating activity in GSTs is essential from the biological and evolutionary perspective.
Methods: In the present investigation an active-site-focused mutant library of GST A2-2 has been screened for enzyme variants with enhanced ITC activity.
Results: Significantly superior activities were found in 34 of the approximately 2000 mutants analyzed, and the majority of the superior GSTs featured His and Gly residues in one of the three active-site positions subjected to mutagenesis.
Conclusions: We explored the propensity of GSTs to obtain altered substrate selectivity and moreover, identified a specific pattern of mutagenesis in GST for enhanced PEITC detoxification, which may play an important role in the evolution of adaptive responses in organisms subjected to ITCs.
General significance: The facile acquisition of enhanced ITC activity demonstrates that this important detoxication function can be promoted by numerous evolutionary trajectories in sequence space.

1. Introduction

Organic isothiocyanates are natural products of wide-ranging interest [1]. They are synthesized and stored as glucosinolates in plants and are released by the action of myrosinase when the plant tissue is damaged. The electrophilic isothiocyanates are toxic and serve to protect plants against invading organisms such as insects and microorganisms. Organic isothiocyanates are detoxified by conjugation with glutathione, which converts the electrophile to a dithiocarbamate in a conjugation reaction catalyzed by glutathione transferases (GSTs) abundantly occurring in the cells of most aerobic organisms. The plant tissues protect themselves against organic isothiocyanates by multiple GSTs, which are expressed in all tissues ranging from roots to leaves [2]. However, herbivores such as insects mount a similar response by producing GSTs as their resistance factors [3]. The biosynthetic pathways to the glucosinolates and isothiocyanates originate from amino acid derivatives and result in large variety of isothiocyanate analogues. From an evolutionary perspective it is therefore of interest to investigate how GST activities can evolve to meet the novel challenges arising from emerging plant isothiocyanates.

It is noteworthy that GST activity with organic isothiocyanates is widely occurring. In the study of two GSTs from cyanobacteria the only prominent activity identified was that with PEITC [4]. In an evolutionary experiment, isothiocyanate activity readily emerged from a GST mutant library [5]. Most higher plants and animals investigated express

Abbreviations: GST, glutathione transferase; GSH, glutathione; AITC, allyl isothiocyanate; BITC, benzyl isothiocyanate; EA, ethacrynic acid; PEITC, phenethyl isothiocyanate; PITC, propyl isothiocyanate; CDNB, 1-chloro-2,4-dinitrobenzene; Non, nonenal; BN, butylnitrite; AD, Δ^5-androstene-3,17-dione; EA, ethacrynic acid; pNPA, p-nitrophenyl acetate; Diiodoethane, 1,2-diiodoethane; CuOOH, cumene hydroperoxide; MD, molecular dynamics

* Corresponding author at: Department of Neurochemistry, Stockholm University, SE-10691 Stockholm, Sweden.
E-mail address: bengt.mannervik@neurochem.su.se (B. Mannervik).

http://dx.doi.org/10.1016/j.bbagen.2014.12.021
0304-4165/

GSTs with isothiocyanate activity. It would appear that there is a close physiological connection between isothiocyanates and GSTs.

The present investigation was designed to explore the propensity of GSTs to evolve altered substrate selectivity for isothiocyanates, which may play an important role in adaptive responses in plants and their cognate herbivores. Three point mutations in the active site of a human GST were investigated in different combinations and the resulting activities with representative GST substrates and alternative isothiocyanate substrates were investigated.

2. Results

2.1. Construction and quality of the focused library of GST A2*E

The H-site of GSTs is responsible for the binding of various electrophilic substrates and thus is hypervariable among different GST species. The H-site of human GST A2*E is composed of 13 amino acid residues, including G10, I12, S14, E104, L107, L108, S110, F111, M208, L213, S216, F220, and F222. Identification of key residues for activity enhancement for a desired substrate is therefore not trivial. However, our previous attempt to enhance GST activity with azathioprine, as a spin-off indicated that three residues (107, 108 and 222) might be important for GSH conjugation with PEITC [6]. Therefore, a focused library targeting these three positions was revisited for isothiocyanate activities. The library stochastically encoded Arg, Asn, Asp, Cys, Gly, His, Ile, Leu, Phe, Ser, Tyr, or Val at each of positions 107 and 108 based on introduction of the NDT codon degeneracy. At position 222 His, Leu, Phe, Pro, Ser, or Tyr were encoded via YHC degeneracy.

2.2. Sequence divergence of A2*E variants with enhanced PEITC activity

Roughly 2000 variant colonies as well as the parent enzyme A2*E colony were picked individually into 96-well plates for growth and lysate preparation. A screening method based on UV/Vis spectroscopy was developed for identifying activity-enhanced variants from the mutant library. By lowering the PEITC concentration to 33 μM, while maintaining the GSH concentration constant at 1 mM, the assay was optimized to distinguish variants with improved enzyme properties from GST A2*E, the starting enzyme. The mean activity of the parent enzyme was 8.24 ($10^{-3}\Delta A_{274}$/min) with a S.D. value of 1.30 ($10^{-3}\Delta A_{274}$/min). Of the enzyme variants investigated 18.9% (355/1881) exhibited improved activity with PEITC, i.e., above the cut-off value of mean + 3 S.D. for the parent enzyme (Fig. 1a).

2.3. Sequence diversity among the high-activity variants

The 34 variants showing activity >20 ($10^{-3}\Delta A_{274}$/min) from the initial screening were sequenced (Fig. 1a), all of which had defined sequences without any spurious mutation introduced during PCR amplification. The variants in the winning pool after screening exhibited high molecular diversity. G and H were over-represented at position 107 and complemented with F and S from the 12 amino acids encoded by NDT randomization. Positions 108 and 222 were highly diversified, with the occurrence of 10 out of 12 possible amino acids encoded by NDT degeneracy and 5 out of 6 using codon YHC, respectively (Fig. 1b). The functional enrichment of G and H at position 107 was then subjected to determination of statistical significance using a binomial test. Both G and H were overwhelmingly dominant with P values of $2.4 * 10^{-10}$ and $2.3 * 10^{-8}$, respectively. To shed light on the over-presentation of G and H in terms of physico-chemical properties at position 107, different quantitative descriptors of amino acids were used for analysis [7–9]. But none of them could explain the under-representation of alternative residues encoded by NDT randomization in this position. It is noteworthy that all GSTs that were highly active with PEITC harbored at least two substitutions at the three targeted positions (Table 1).

2.4. Characterization of the most active variants

The six variants with the highest elevated activity with PEITC were then subjected to specific activity determinations with various substrates in order to obtain an overall picture of enzyme performance in the multi-dimensional chemical-reaction space [6,10]. All of them showed increased specific activity with PEITC by a factor from 8.1 to 17.1 fold as compared to the parent GST A2*E (Fig. 2a). The specific activities with CDNB, butylnitrite and CuOOH, relative to A2*E, changed modestly within in the range from 0.26 to 1.69 fold, while the differences relative to A2*E in the remaining substrates varied up to 15 fold. It was interesting to find that all the selected variants displayed enhanced activities with nonenal and EA, considering the fact that the molecular structures of nonenal and EA are quite different from those of PEITC. On the other hand, both nonenal and EA are alkenes, which undergo addition reactions with the sulfur of glutathione, a chemical transformation initiated by nucleophilic attack on an sp^2-hybridized carbon, with mechanistic similarities to the ITC reaction.

A set of isothiocyanate compounds occurring in human diets was then used for more detailed steady-state kinetic studies of the enzyme variants. Three naturally-occurring isothiocyanates besides PEITC (in watercress and garden cress) were used for characterization, namely, BITC (in red cabbage), AITC (in cabbage, mustard, and horseradish) and PITC (in rapeseeds) [11]. For the reaction with PEITC, all the selected variants displayed >30 fold increases in catalytic efficiencies (Fig. 2b). The enhancement in performance stemmed from both increases in k_{cat} and decreases in K_M values. HLP, the most active variant with PEITC, exhibited catalytic efficiency of 625 $mM^{-1}\cdot s^{-1}$, with a 43-fold increase compared to that of the parent enzyme. The k_{cat} of HLP with PEITC increased from 1.71 to 14.8 s^{-1}, while K_M was lowered from 0.12 to

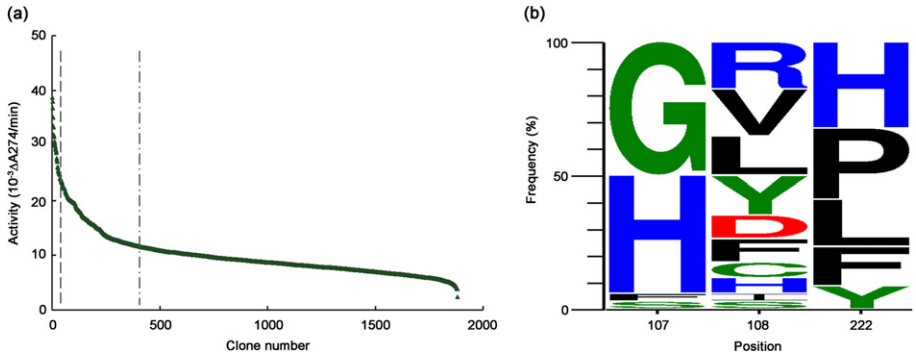

Fig. 1. (a). Activity values of crude bacterial cell lysates containing GST A2*E variants in twenty 96-well microtiter plates in descending order of PEITC activity. Variants exhibiting activity above 12.1 ($10^{-3}\Delta A_{274}$/min) (left of the dot-dashed line vertical line) are considered as variants with improved PEITC activity and variants with activity above 20 ($10^{-3}\Delta A_{274}$/min) (left of the dashed vertical line) were taken for sequence analysis. (b). A WebLogo [55] representation of substitution patterns in the three randomized positions among the high-activity GST variants. The font height of the letter is proportional to the frequency of amino acid residue appearance at each corresponding position.

Table 1
Specific activities of GST A2-2 variants with alternative substrates. Values (means ± s.d., n = 3) were determined as described in the Material and methods section.

GST variants	CDNB	Non	BN	AD	EA	pNPA	Diiodoethane	PEITC	CuOOH
	μmol·min^{-1}·mg^{-1}								
A2*E	14.4 ± 0.2	0.11 ± 0.01	91.7 ± 1.2	0.0090 ± 0.0008	0.061 ± 0.005	0.55 ± 0.01	299.8 ± 6.9	3.41 ± 0.45	5.59 ± 0.05
HFF	16.1 ± 0.6	0.94 ± 0.08	54.5 ± 0.3	0.0545 ± 0.0014	0.135 ± 0.006	0.29 ± 0.003	28.1 ± 0.7	29.2 ± 2.0	8.81 ± 0.00
HYL	8.3 ± 0.2	1.15 ± 0.06	62.9 ± 0.7	0.0216 ± 0.0004	0.100 ± 0.016	0.19 ± 0.003	41.4 ± 1.2	27.7 ± 0.01	5.98 ± 0.16
HLP	10.3 ± 0.8	1.33 ± 0.13	53.6 ± 0.6	0.0026 ± 0.0002	0.200 ± 0.020	0.039 ± 0.010	100.6 ± 0.1	34.3 ± 0.4	5.08 ± 0.15
GLH	7.2 ± 0.2	0.38 ± 0.01	23.6 ± 0.2	0.0180 ± 0.0003	0.344 ± 0.009	0.038 ± 0.003	52.0 ± 0.8	25.0 ± 0.6	2.32 ± 0.03
HLH	5.0 ± 0.1	1.44 ± 0.10	30.2 ± 0.2	0.0026 ± 0.0003	0.275 ± 0.019	0.091 ± 0.001	107.0 ± 0.4	58.2 ± 1.2	3.33 ± 0.04
GRF	24.4 ± 0.6	0.57 ± 0.01	33.8 ± 0.3	0.0933 ± 0.0027	0.323 ± 0.029	0.224 ± 0.003	41.5 ± 1.0	28.3 ± 0.9	3.60 ± 0.08

0.024 mM. Interestingly, all the selected variants also displayed increases of the same magnitude in catalytic efficiencies with BITC, and their ranking in terms of BITC activity was the same as for PEITC. The catalytic efficiencies with AITC and PITC were two orders of magnitude lower than those of PEITC and BITC, within only a two-fold difference in absolute values.

*2.5. Modeling of GST A2*E, and mutants HLP and GRF docked with PEITC and BITC*

To structurally characterize the most active mutants, HLP and GRF, we performed a modeling study of these variants and GST A2*E complexed with the isothiocyanates PEITC and BITC. GST A2*E, HLP, and

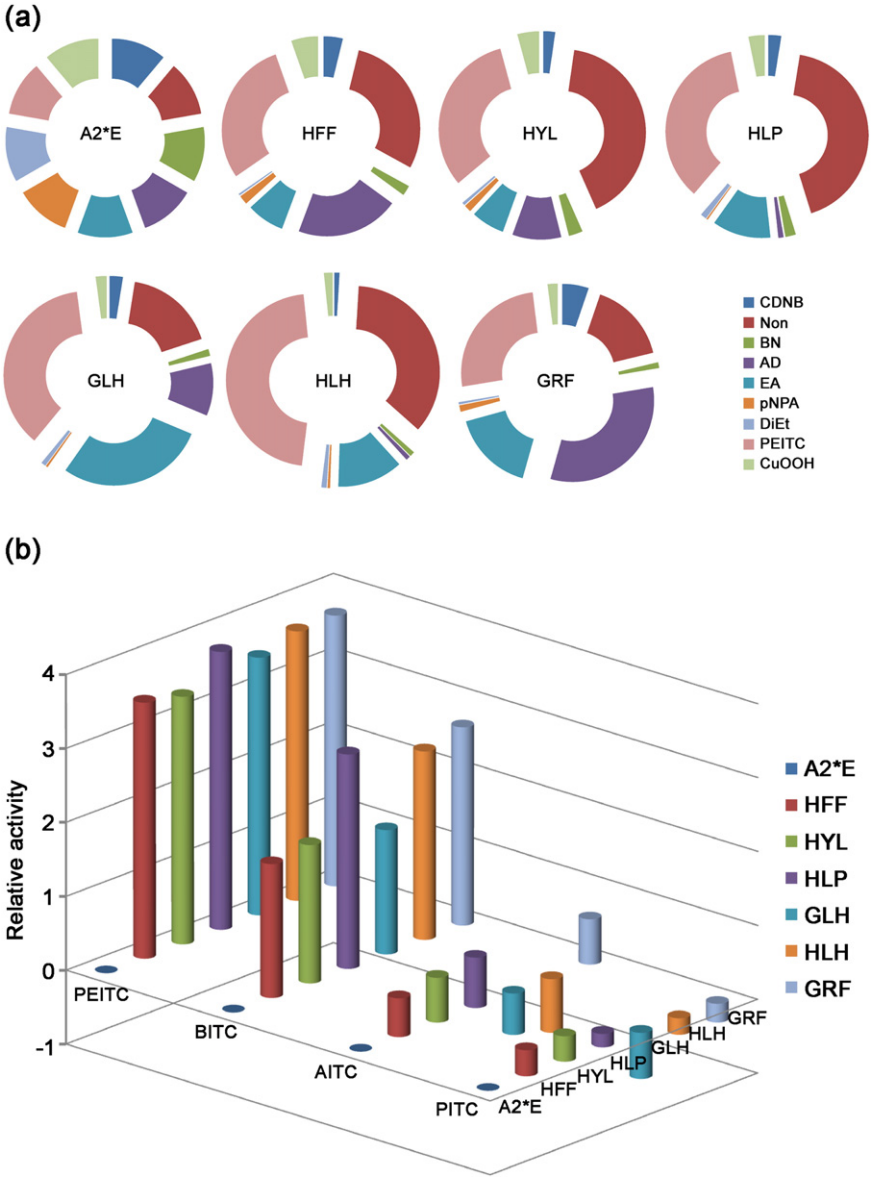

Fig. 2. (a). Exploded-doughnut chart of relative specific activities of various substrates for selected variants. The specific activity of a given substrate was normalized to the activity of A2*E with the same substrate. (b). Bar plot demonstrating the relative catalytic efficiencies of selected variants with representative ITCs compared to efficiency of the parent enzyme GST A2*E. Ratios of catalytic efficiencies are transformed to natural logarithm of k_{cat}/K_M (mut) divided by k_{cat}/K_M (A2*E) for ease of visualization.

GRF models were submitted to MD simulations to obtain a more realistic disposition of the mutated residues. Subsequently, PEITC and BITC were docked to the MD reference structure of each model, respectively (Figs. 3 and 4).

We observed that with the same enzyme variant the two isothiocyanates had a similar spatial arrangement. This is in accordance with the similar effects of the mutations on the catalytic efficiencies noted for the two substrates (Table 2). In fact, PEITC and BITC are structurally similar, both having a benzene ring and an N═C═S functional group. However, between the three enzyme variants the positioning of the substrates changed considerably. For GST A2*E the benzene group of the substrates was placed in the interface of the G-site with the H-site interacting with F222, while the N of the N═C═S group was hydrogen-bonded with the R15 side chain (Fig. 3). In the HLP and GRF variants, L107 was mutated to H and G, respectively, which in both cases resulted in an opening of the H-site. The bulky benzene group of the substrates was therefore allowed to strongly interact through London dispersion forces with the hydrophobic core of the H-site, explaining the lower K_M values for the two variants compared with GST A2*E (Table 2). This arrangement was however different in the two variants mainly due to the different residues in positions 222 and 108. In HLP, P222 was involved in a CH/π interaction with F111, and the benzene group of both substrates interacted with L108 and established a strong T-shaped π-stacking with F111 (Fig. 4a). On the other hand, in the H-site of GRF we observed a T-shape π-stacking between F111 and F222. When GRF was complexed with PEITC, the benzene ring established a strong parallel-displaced π-stacking with F111. However, when GRF was complexed with BITC a less strong sandwich π-stacking with F111 was observed (Fig. 4b), which seemed to be in accordance with a lower K_M value for PEITC than for BITC (Table 2). Moreover, in the HLP and GRF variants the sulfur of the substrate N═C═S group was hydrogen bonded to the GSH main chain (Fig. 4).

2.6. Predicted thermostability changes in the selected variants

Changes of Gibbs free energy of folding were computationally obtained by FoldX [12]. All variants were predicted to have decreased folding stability compared to the parent enzyme GST A2*E after the introduction of hydrophilic or even charged amino acid residues in the hydrophobic active site of GST, as a result of the overwhelming presence of destabilizing mutations [13]. $\Delta\Delta G_{folding}$ values among the selected variants varied from 3.51 to 6.54 kcal/mol. The overall impact of mutations on the calculated thermostability was 2.34 kcal/mol per mutation, close to our previous calculations and experimental observations [6].

3. Discussion

3.1. Isothiocyanates are phytochemical inducers and substrates of GSTs

A variety of organic isothiocyanates are secondary metabolites in plants, with cruciferous vegetables as particularly rich sources, enzymatically released from corresponding glucosinolates with the aid of myrosinase. In fact, ITCs have drawn major attention from nutritionists for decades because of their potential chemoprotective effects against cancer [14–16], cardiovascular diseases [17], neurodegeneration [18], and even the development of diabetes [19]. Although ITCs are mostly credited for their chemoprotective activities against chronic degenerative diseases, they are also regarded as potentially genotoxic compounds due to their ability to form DNA adducts [20].

The chemoprotective effects of ITCs are commonly attributed to the inhibition of phase I cytochrome P450 (CYP) drug-metabolizing enzymes and induction of phase II drug-metabolizing enzymes, effected by the sulfur-containing N═C═S functional group [21,22]. The enzyme activity of CYPs is inhibited by various types of mechanisms at different molecular levels, including gene transcription and enzymatic actions. By contrast, both in vitro and in vivo data strongly suggest that expression of detoxication enzymes such as GSTs, facilitating the inactivation and excretion of toxic xenobiotics, can be significantly induced by ITCs [23–25]. The signaling pathways and molecular mechanisms of detoxification enzyme induction modulated by ITCs have been well reviewed elsewhere [26,27].

In addition to functioning as phytochemical inducers of GSTs, ITCs belong to the group of a few verified natural substrates for GSTs. However, different GSTs exhibit diverging catalytic efficiencies with ITCs occurring in plants [28,29], which may have consequences for the outcome of dietary cancer chemoprevention [30]. The complex interaction between ITCs and GSTs actually makes it a natural model to study substrate induction of detoxication enzymes.

3.2. Screening of the library with PEITC

Although active-site reengineering aimed at alteration of substrate specificity has been successfully achieved in various enzyme systems, the prediction of appropriate mutations at the right positions is still

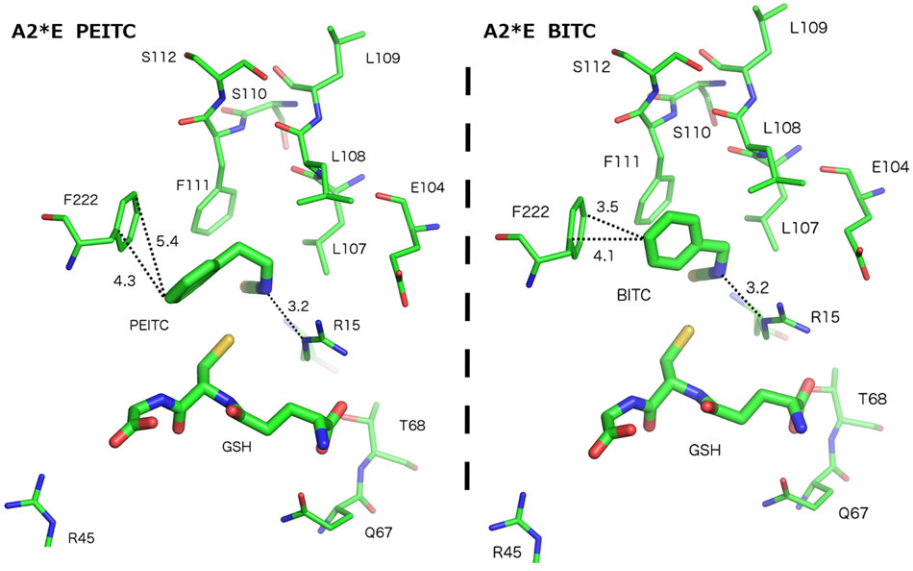

Fig. 3. Active-site of the MD GST A2*E reference structure. On the left GST A2*E is complexed with PEITC and GSH, while on the right it is complexed with BITC and GSH. Distances are shown in Å units.

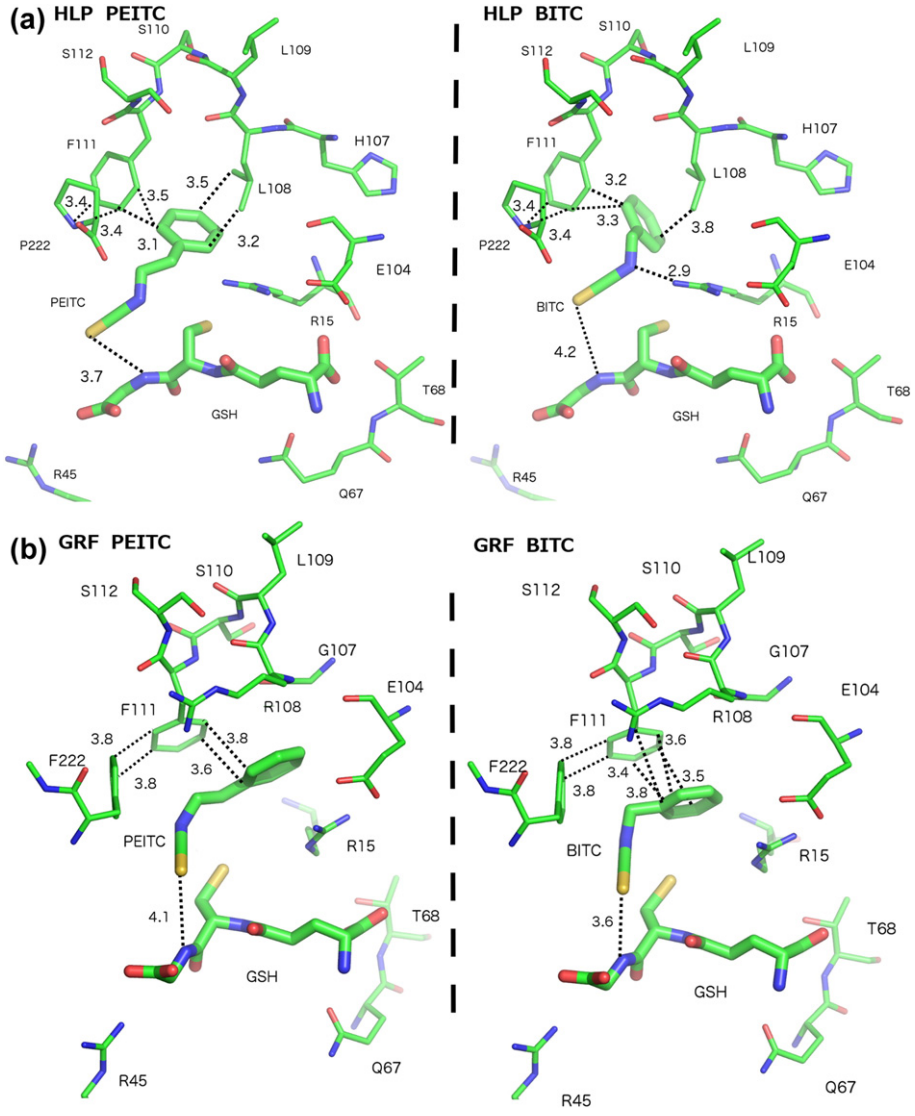

Fig. 4. (a). Active-site of the HLP mutant structure. On the left HLP is modeled with PEITC and GSH, while on the right it is modeled with BITC and GSH. (b). Active-site of the GRF mutant structure. On the left it is modeled with PEITC and GSH, while on the right it is modeled with BITC and GSH. Distances are shown in Å units.

Table 2
Steady-state kinetic parameters of GST A2-2 variants with alternative isothiocyanate substrates. Initial velocity data were fitted with the Michaelis–Menten equation using nonlinear regression analysis. k_{cat} values are expressed for each subunit. Changes of Gibbs free energy of folding were computationally determined by FoldX.

GST variants	$\Delta\Delta G_{folding}$ (kcal·mol^{-1})	PEITC			BITC		
		k_{cat} (S^{-1})	K_M (mM)	k_{cat}/K_M ($mM^{-1}\cdot S^{-1}$)	k_{cat} (S^{-1})	K_M (mM)	k_{cat}/K_M ($mM^{-1}\cdot S^{-1}$)
A2*E	0	1.71 ± 0.07	0.12 ± 0.01	14.5	1.83 ± 0.23	0.084 ± 0.024	21.7
HFF	3.51	10.9 ± 0.49	0.023 ± 0.004	464.6	25.4 ± 3.4	0.19 ± 0.04	133.0
HYL	5.66	9.39 ± 0.58	0.023 ± 0.006	413.0	16.6 ± 2.6	0.12 ± 0.04	141.0
HLP	5.88	14.8 ± 0.70	0.024 ± 0.005	624.8	9.05 ± 1.20	0.023 ± 0.010	395.6
GLH	6.54	9.08 ± 0.45	0.019 ± 0.004	474.2	223.5 ± 211.4	1.92 ± 2.22	116.6
HLH	4.50	17.4 ± 1.16	0.031 ± 0.008	557.8	59.9 ± 12.8	0.22 ± 0.07	278.5
GRF	4.32	10.2 ± 0.21	0.018 ± 0.002	567.9	21.3 ± 2.3	0.067 ± 0.017	317.1
GST variants	$\Delta\Delta G_{folding}$ (kcal·mol^{-1})	AITC			PITC		
		k_{cat} (S^{-1})	K_M (mM)	k_{cat}/K_M ($mM^{-1}\cdot S^{-1}$)	k_{cat} (S^{-1})	K_M (mM)	k_{cat}/K_M ($mM^{-1}\cdot S^{-1}$)
A2*E	0	0.91 ± 0.04	1.01 ± 0.20	0.91	2.08 ± 0.23	0.72 ± 0.15	2.90
HFF	3.51	0.47 ± 0.03	0.31 ± 0.07	1.54	4.64 ± 0.28	1.12 ± 0.11	4.13
HYL	5.66	1.02 ± 0.05	0.61 ± 0.17	1.67	5.03 ± 0.46	1.23 ± 0.17	4.10
HLP	5.88	1.43 ± 0.05	0.80 ± 0.25	1.8	5.34 ± 0.66	1.54 ± 0.28	3.48
GLH	6.54	0.57 ± 0.02	1.10 ± 0.19	0.52	4.49 ± 1.25	2.89 ± 1.01	1.55
HLH	4.50	0.28 ± 0.03	0.63 ± 0.06	0.44	3.36 ± 0.41	1.45 ± 0.24	2.32
GRF	4.32	0.90 ± 0.02	0.53 ± 0.24	1.68	5.24 ± 1.37	2.33 ± 0.80	2.25

not trivial considering the fact that the volume of active site comprises somewhat about 10–20% of the total enzyme molecule [31,32]. In a previous study, we integrated molecular docking and proposed reaction mechanism into a general approach for the construction of a high-quality focused mutant library of human GST A2-2 [33]. The best mutant in the library, a triple mutant (L107G/L108D/F222H) of GST A2-2*E approached the upper limit of activity of the GST scaffold toward our target substrate azathioprine. This GST mutant also showed significant enhancement of the activity with PEITC [6], which differs with azathioprine in several aspects including chemical structure and reaction mechanism (addition versus substitution). Thus, we decided to take a retrospective look at the performance of the library on detoxication of organic isothiocyanates.

Since at least two A2*E variants investigated in the previous study exhibited significantly enhanced activity with PEITC [6], we decided to use PEITC as a model substrate for screening. Hit identification was based on preliminary screening of crude lysates, which depends on multiple factors, such as expressivity of the target proteins, contents in crude extracts, assay conditions and intrinsic enzymatic activities. By optimizing the PEITC concentration in the assay, a significant difference in spectroscopic signal between wild-type A2*E and the GDH variant was achieved. The focused library of GST A2*E was thus screened successfully under these conditions (Fig. 1a).

Although k_{cat} and k_{cat}/K_M values of A2*E and GDH differed over 22 fold [6], the signals based on the current settings of screening differed only by 3 times (8.24 compared to $24.3 \times 10^{-3}\Delta A_{274}$/min). A cut-off value of 20 ($10^{-3}\Delta$A274/min) to distinguish activity-enhanced variants from the less active enzyme variants was determined and a total of 34 variants were considered as hits for sequence analysis.

3.3. Natural diversity of residue 107 in homologous GST A2-2 sequences

A total of five hundred sequences homologous to GST A2-2 (data obtained from protein Blast searches) were aligned with ClustalW2 [34] using the software default parameters to understand the natural diversity of residue 107 of human GST A2-2 among its homologs. Since plant GSTs are only distantly related to mammalian GSTs, the majority of human GST A2-2 homologs belonged to the category of animals with the remaining minority belonging to cellular slime molds, ciliates, apicomplexans, choanoflagellates or even bacteria. H at the position corresponding to residue 107 in human GST A2-2 was found to exist in graminivores, such as gorilla, chimpanzee, macaca, horse, cow, and sheep. This observation suggests evolutionary and functional importance of H at this specific position in herbivores.

Previously our laboratory and other research groups explored the use of reduced amino acid alphabets in randomized positions only including amino acids found in naturally occurring homologous proteins, to minimize the number of variants in the selection/screening effort of directed evolution [35,36]. Although the strategy has been found useful for finding desired mutants, in our current case, we did not observe any naturally occurring human GST A2-2 homolog displaying G at position 107 in spite of its abundance in the screening of the mutant library. It thus appears that potentially advantageous mutations can be missed if the mutagenesis incorporates only the natural diversity observed.

3.4. Role of active-site structure on catalytic activity with ITCs

In the present investigation, we successfully evolved GST activity with PEITC from A2*E up to 43 fold in terms of catalytic efficiency from a small focused library. A total of 355, corresponding to 19% of the variants in the libraries, displayed enhanced activities with PEITC. Since crude lysate was used for the initial screening, confounding factors such as enzyme expressivity, stability and even the extent of cell lysis and protein retrieval could lead to false hits. Interestingly, all the mutants subjected to detailed kinetic studies were predicted to have impaired thermostability and significant increases in terms of catalytic efficiencies with the screening substrate, PEITC. For detoxication enzymes, such as GSTs and CYP450, which have evolved for millions of years to bind and metabolize a wide range of diverse substrates, conformational diversity appears favored for enzyme–substrate complementarity at the cost of stability. Based on studies of two structurally related GST isoenzymes, GST A1-1 and GST A4-4, with very different promiscuity profiles, it has been suggested that functional promiscuity stems from enzyme global flexibility [37–39]. Moreover, stability toward urea denaturation was shown to be negatively correlated with functional promiscuity.

In summary, we explored the propensity of GSTs to altered substrate selectivity and moreover, identified a specific pattern of mutagenesis in GST for enhanced PEITC detoxification, which may play an important role in adaptive responses in plants and their predators.

4. Materials and methods

4.1. Reagents

Pfu DNA polymerase and *Dpn*I restriction enzyme were purchased from Fermentas. QIAquick gel extraction kit was from Qiagen. Oligonucleotides used were ordered from Thermo Fisher Scientific. *Escherichia coli* XL1-Blue obtained from Stratagene was used for protein expression. Nunc 96-well microplates were from Thermo Scientific. Cumene hydroperoxide and Δ^5-androstene-3,17-dione were obtained from Fluka and Steraloids Inc., respectively. Other chemicals were from Sigma-Aldrich.

4.2. Library construction

DNA encoding human GST A2-2 allelic variant E (GST A2*E), cloned in the pGΔETac vector [40], was used as a template for focused library construction. The focused mutant library was constructed by a dual-tube approach as reported previously [33]. All proteins were expressed as N-terminus polyhistidine-tagged proteins for ease of purification. The quality of the mutant library was checked by sequencing randomly picked colonies after transformation into *E. coli* XL1-Blue.

4.3. Screening in 96-well microplates

After quality confirmation of the mutant library, randomly picked colonies were individually grown in 250 μl LB media supplemented with 100 $\mu g \cdot ml^{-1}$ ampicillin for 16 h at 37 °C in 96-well plates. 2 μl overnight LB culture was inoculated into 250 μl 2 × YT culture containing 100 $\mu g \cdot ml^{-1}$ ampicillin for each single well. Target enzymes were overexpressed with shaking for 20 h at 30 °C, in the absence of IPTG induction. Cells were then pelleted by centrifugation at 3500 *g* for 15 min. The pellets were then subjected to lysis by lysozyme (200 $\mu g \cdot ml^{-1}$) in NaPi buffer (pH 7.0). After shaking the microplates at 50 rpm on ice for 1 h, three rounds of freezing–thawing were performed for complete lysis (10 min at −80 °C, followed by 4 min at 37 °C with shaking at 200 rpm). The lysate was clarified by centrifugation at 4000 *g* for 60 min and used for assay in 250-μl reactions at 30 °C according to Kolm et al. [28]. Briefly, GSH concentration was constant at 1 mM, while PEITC concentration was set at 33 μM. All measurements were performed in duplicate and mean values were subjected to further analysis for hit identification.

4.4. Expression and purification of GST A2*E variants

After screening for PEITC activity, GST variants exhibiting significantly enhanced activity were chosen for large-scale expression. Single colonies with GST A2*E variant coding sequences in pGΔETac were cultured in LB media with ampicillin at 37 °C. Overnight cultures were diluted 100-fold in 500 ml 2 × YT medium containing ampicillin. Overexpression of the target enzymes were induced at 30 °C for 20 h by adding 0.2 mM isopropyl-β-D-thiogalactoside (IPTG) when OD_{600}

reached 0.3. Cells were harvested by centrifugation and lysed by constant cell disruption systems at 20 kpsi. After centrifugation, clarified cell culture supernatants were filtered through 0.45 μm nylon membrane filters prior to loading the samples into the His GraviTrap™ columns. Purification was performed according to the manufacturer's instructions. After overnight dialysis in Tris–EDTA–mercaptoethanol buffer, the purity of the purified enzymes was assessed by SDS-PAGE. The protein concentrations were further determined by Bradford assay, using bovine serum albumin as a standard.

4.5. Kinetic studies

GSH conjugation reactions were investigated at 30 °C in 100 mM NaP_i buffer in a Shimadzu UV2501-PC spectrophotometer. Further details on the measurement of specific activities and steady-state kinetics can be found elsewhere [41].

4.6. Estimating the effects of mutations on thermostability

The changes of thermostability caused by mutations at positions 107, 108 and 222 were calculated with FoldX [12]. First, the 3D structure of glutathione transferase A2-2 in complex with glutathione (2WJU) was optimized by the repair function of FoldX. Secondly, the optimized structure was used as a template for the production of structural models of mutants with the BuildModel command. Thirdly, energies for all the variants were calculated by the energy calculation function, and the effects of corresponding mutations on thermostability were estimated by subtracting the values from that of human GST A2*E. Fourthly, realistic energy values were deduced by the correlation function between experimental and calculated data ($\Delta\Delta G^{Experimental} = (\Delta\Delta G^{FoldX} + 0.078) / 1.14$) [42].

4.7. Molecular dynamics simulations

A model of GST A2*E was obtained by mutating P110S and T112S in the wild-type allelic variant C (GSTA2*C) (PDB number: 2WJU). Positions 107, 108 and 222 of GST A2*E were further mutated to obtain modeled structures of HLP and GRF. Then the three models were submitted to MD simulations. Charges of the glutathione molecule were based on Dourado et al. [43], while dihedrals, angles, bonds, and van der Waals parameters were obtained in the Amber99 force field [44,45]. All the modeled structures were solvated with single point charge (SPC) [46] waters. The three model systems were submitted to 100 steps of steepest descent energy minimization to remove bad contacts between the solvent and the protein and later equilibrated with a 200 ps restrained MD simulation to relax the water molecules. For all systems, production simulations were run for 20 ns using a time step of 0.002 ps, with the trajectories saved at each 20 ps. The temperature and pressure were maintained constant by the use of a v-rescale thermostat [47] and a Parrinello-Rahman barostat [48] (parameters: $\tau_T = 0.1$ ps, $T_{ref} = 300$ K, $P_{ref} = 1$ bar). The particle mesh Ewald (PME) [49] method was applied to compute electrostatic interactions with a cut-off of 1.0 nm. A twin range cut-off with a neighbor list cut-off 1.0 and a cut-off of 1.0 was used for the van der Waals interactions. Periodic boundary conditions were used in all simulations. All the bonds involving hydrogen atoms were kept fixed by the LINCS constraint algorithm [50]. All simulations and analyses were carried out using the Gromacs 4.6.5 software package conjugated with the PARM99 force field [44–45, 51–53].

4.8. Molecular docking

For each model a reference structure of the 20 ns MD simulation, which corresponds to the one more similar to the average structure, was used to dock the substrates. The docking of PEITC and BITC substrates was performed with AutoDock 4.2 [54]. The substrates were maintained flexible while the enzyme structures were kept rigid. The grid was centered on the active site (G-site and H-site) of GSTs. The population was 150, the maximum number of generations was 27,000 and the maximum number of energy evaluations was 250,000. For each system, the docked structure with the best binding energy was chosen.

Acknowledgements

This work was supported by the Swedish Research Council and the Swedish Cancer Society.

References

[1] Y. Zhang, P. Talalay, Anticarcinogenic activities of organic isothiocyanates: chemistry and mechanisms, Cancer Res. 54 (1994) 1976s–1981s.
[2] E. Nutricati, A. Miceli, F. Blando, L. De Bellis, Characterization of two *Arabidopsis thaliana* glutathione S-transferases, Plant Cell Rep. 25 (2006) 997–1005.
[3] F. Francis, N. Vanhaelen, E. Haubruge, Glutathione S-transferases in the adaptation to plant secondary metabolites in the *Myzus persicae* aphid, Arch. Insect Biochem. Physiol. 58 (2005) 166–174.
[4] E. Wiktelius, G. Stenberg, Novel class of glutathione transferases from cyanobacteria exhibit high catalytic activities towards naturally occurring isothiocyanates, Biochem. J. 406 (2007) 115–123.
[5] A. Runarsdottir, B. Mannervik, A novel quasi-species of glutathione transferase with high activity towards naturally occurring isothiocyanates evolves from promiscuous low-activity variants, J. Mol. Biol. 401 (2010) 451–464.
[6] W. Zhang, D.F. Dourado, P.A. Fernandes, M.J. Ramos, B. Mannervik, Multidimensional epistasis and fitness landscapes in enzyme evolution, Biochem. J. 445 (2012) 39–46.
[7] S. Hellberg, M. Sjostrom, B. Skagerberg, S. Wold, Peptide quantitative structure–activity relationships, a multivariate approach, J. Med. Chem. 30 (1987) 1126–1135.
[8] M. Sandberg, L. Eriksson, J. Jonsson, M. Sjostrom, S. Wold, New chemical descriptors relevant for the design of biologically active peptides. A multivariate characterization of 87 amino acids, J. Med. Chem. 41 (1998) 2481–2491.
[9] W. Braun, M.S. Venkatarajan, New quantitative descriptors of amino acids based on multidimensional scaling of a large number of physical–chemical properties, J. Mol. Model. 7 (2001) 445–453.
[10] S. Kurtovic, B. Mannervik, Identification of emerging quasi-species in directed enzyme evolution, Biochemistry 48 (2009) 9330–9339.
[11] K.L. Cheung, A.N. Kong, Molecular targets of dietary phenethyl isothiocyanate and sulforaphane for cancer chemoprevention, AAPS J. 12 (2010) 87–97.
[12] R. Guerois, J.E. Nielsen, L. Serrano, Predicting changes in the stability of proteins and protein complexes: a study of more than 1000 mutations, J. Mol. Biol. 320 (2002) 369–387.
[13] N. Tokuriki, F. Stricher, L. Serrano, D.S. Tawfik, How protein stability and new functions trade off, PLoS Comput. Biol. 4 (2008) e1000002.
[14] S.S. Hecht, Chemoprevention by isothiocyanates, J. Cell. Biochem. Suppl. 22 (1995) 195–209.
[15] S.L. Navarro, F. Li, J.W. Lampe, Mechanisms of action of isothiocyanates in cancer chemoprevention: an update, Food Funct. 2 (2011) 579–587.
[16] S.V. Singh, K. Singh, Cancer chemoprevention with dietary isothiocyanates mature for clinical translational research, Carcinogenesis 33 (2012) 1833–1842.
[17] P.M. Kris-Etherton, K.D. Hecker, A. Bonanome, S.M. Coval, A.E. Binkoski, K.F. Hilpert, A.E. Griel, T.D. Etherton, Bioactive compounds in foods: their role in the prevention of cardiovascular disease and cancer, Am. J. Med. 113 (Suppl. 9B) (2002) 71S–88S.
[18] A.T. Dinkova-Kostova, R.V. Kostov, Glucosinolates and isothiocyanates in health and disease, Trends Mol. Med. 18 (2012) 337–347.
[19] M.Y. Song, E.K. Kim, W.S. Moon, J.W. Park, H.J. Kim, H.S. So, R. Park, K.B. Kwon, B.H. Park, Sulforaphane protects against cytokine- and streptozotocin-induced beta-cell damage by suppressing the NF-kappaB pathway, Toxicol. Appl. Pharmacol. 235 (2009) 57–67.
[20] C. Fimognari, E. Turrini, L. Ferruzzi, M. Lenzi, P. Hrelia, Natural isothiocyanates: genotoxic potential versus chemoprevention, Mutat. Res. 750 (2012) 107–131.
[21] P. Talalay, J.W. Fahey, Phytochemicals from cruciferous plants protect against cancer by modulating carcinogen metabolism, J. Nutr. 131 (2001) 3027S–3033S.
[22] S.E. Steck, J.R. Hebert, GST polymorphism and excretion of heterocyclic aromatic amine and isothiocyanate metabolites after *Brassica* consumption, Environ. Mol. Mutagen. 50 (2009) 238–246.
[23] J.J. Bogaards, H. Verhagen, M.I. Willems, G. van Poppel, P.J. van Bladeren, Consumption of Brussels sprouts results in elevated alpha-class glutathione S-transferase levels in human blood plasma, Carcinogenesis 15 (1994) 1073–1075.
[24] J.W. Lampe, C. Chen, S. Li, J. Prunty, M.T. Grate, D.E. Meehan, K.V. Barale, D.A. Dightman, Z. Feng, J.D. Potter, Modulation of human glutathione S-transferases by botanically defined vegetable diets, Cancer Epidemiol. Biomarkers Prev. 9 (2000) 787–793.
[25] Y. Zhang, R. Munday, H.E. Jobson, C.M. Munday, C. Lister, P. Wilson, J.W. Fahey, P. Mhawech-Fauceglia, Induction of GST and NQO1 in cultured bladder cells and in the urinary bladders of rats by an extract of broccoli (*Brassica oleracea italica*) sprouts, J. Agric. Food Chem. 54 (2006) 9370–9376.
[26] E.D. Owuor, A.N. Kong, Antioxidants and oxidants regulated signal transduction pathways, Biochem. Pharmacol. 64 (2002) 765–770.

[27] W.D. Holtzclaw, A.T. Dinkova-Kostova, P. Talalay, Protection against electrophile and oxidative stress by induction of phase 2 genes: the quest for the elusive sensor that responds to inducers, Adv. Enzyme Regul. 44 (2004) 335–367.
[28] R.H. Kolm, U.H. Danielson, Y. Zhang, P. Talalay, B. Mannervik, Isothiocyanates as substrates for human glutathione transferases: structure–activity studies, Biochem. J. 311 (1995) 453–459.
[29] Y. Zhang, R.H. Kolm, B. Mannervik, P. Talalay, Reversible conjugation of isothiocyanates with glutathione catalyzed by human glutathione transferases, Biochem. Biophys. Res. Commun. 206 (1995) 748–755.
[30] A. Seow, C.Y. Shi, F.L. Chung, D. Jiao, J.H. Hankin, H.P. Lee, G.A. Coetzee, M.C. Yu, Urinary total isothiocyanate (ITC) in a population-based sample of middle-aged and older Chinese in Singapore: relationship with dietary total ITC and glutathione S-transferase M1/T1/P1 genotypes, Cancer Epidemiol. Biomarkers Prev. 7 (1998) 775–781.
[31] P.V. Kostetsky, Location and volume of the active site of chymotrypsin, Biochem. Biokhim. 72 (2007) 392–397.
[32] V.S. Bhatt, C.Y. Guo, W. Guan, G. Zhao, W. Yi, Z.J. Liu, P.G. Wang, Altered architecture of substrate binding region defines the unique specificity of UDP-GalNAc 4-epimerases, Protein Sci. 20 (2011) 856–866.
[33] W. Zhang, O. Moden, K. Tars, B. Mannervik, Structure-based redesign of GST A2-2 for enhanced catalytic efficiency with azathioprine, Chem. Biol. 19 (2012) 414–421.
[34] M.A. Larkin, G. Blackshields, N.P. Brown, R. Chenna, P.A. McGettigan, H. McWilliam, F. Valentin, I.M. Wallace, A. Wilm, R. Lopez, J.D. Thompson, T.J. Gibson, D.G. Higgins, Clustal W and Clustal X version 2.0, Bioinformatics 23 (2007) 2947–2948.
[35] H. Jochens, U.T. Bornscheuer, Natural diversity to guide focused directed evolution, ChemBioChem 11 (2010) 1861–1866.
[36] S. Sun, W. Zhang, B. Mannervik, D.I. Andersson, Evolution of broad spectrum beta-lactam resistance in an engineered metallo-beta-lactamase, J. Biol. Chem. 288 (2013) 2314–2324.
[37] L. Hou, M.T. Honaker, L.M. Shireman, L.M. Balogh, A.G. Roberts, K.C. Ng, A. Nath, W.M. Atkins, Functional promiscuity correlates with conformational heterogeneity in A-class glutathione S-transferases, J. Biol. Chem. 282 (2007) 23264–23274.
[38] M.T. Honaker, M. Acchione, J.P. Sumida, W.M. Atkins, Ensemble perspective for catalytic promiscuity: calorimetric analysis of the active site conformational landscape of a detoxification enzyme, J. Biol. Chem. 286 (2011) 42770–42776.
[39] M.T. Honaker, M. Acchione, W. Zhang, B. Mannervik, W.M. Atkins, Enzymatic detoxication, conformational selection, and the role of molten globule active sites, J. Biol. Chem. 288 (2013) 18599–18611.
[40] M. Widersten, B. Mannervik, Glutathione transferases with novel active sites isolated by phage display from a library of random mutants, J. Mol. Biol. 250 (1995) 115–122.
[41] A. Shokeer, A.K. Larsson, B. Mannervik, Residue 234 in glutathione transferase T1-1 plays a pivotal role in the catalytic activity and the selectivity against alternative substrates, Biochem. J. 388 (2005) 387–392.
[42] N. Tokuriki, D.S. Tawfik, Chaperonin overexpression promotes genetic variation and enzyme evolution, Nature 459 (2009) 668–673.
[43] D.F. Dourado, P.A. Fernandes, B. Mannervik, M.J. Ramos, Glutathione transferase: new model for glutathione activation, Chem. Eur. J. 14 (2008) 9591–9598.
[44] W.D. Cornell, P. Cieplak, C.I. Bayly, I.R. Gould, K.M. Merz, D.M. Ferguson, D.C. Spellmeyer, T. Fox, J.W. Caldwell, P.A. Kollman, A second generation force field for the simulation of proteins, nucleic acids, and organic molecules (vol 117, pg 5179–5197, 1995), J. Am. Chem. Soc. 118 (1996) 2309.
[45] J.M. Wang, R.M. Wolf, J.W. Caldwell, P.A. Kollman, D.A. Case, Development and testing of a general amber force field (vol 25, pg 1157–1174, 2004), J. Comp. Chem. 26 (2005) 114.
[46] H. Berendsen, J.P.M. Postma, W.F. vanGunsteren, Intermolecular Forces, D. Reidel Publishing Company, Dordrecht, 1981.
[47] G. Bussi, D. Donadio, M. Parrinello, Canonical sampling through velocity rescaling, J. Chem. Phys. 126 (2007).
[48] M. Parrinello, A. Rahman, Polymorphic transitions in single-crystals — a new molecular-dynamics method, J. Appl. Phys. 52 (1981) 7182–7190.
[49] U. Essmann, L. Perera, M.L. Berkowitz, T. Darden, H. Lee, L.G. Pedersen, A smooth particle mesh Ewald method, J. Chem. Phys. 103 (1995) 8577–8593.
[50] B. Hess, H. Bekker, H. Berendsen, J. Fraaije, LINCS: a linear constraint solver for molecular simulations, J. Comp. Chem. 18 (1997) 1463–1472.
[51] E. Lindahl, B. Hess, D. Van der Spoel, GROMACS 3.0: a package for molecular simulation and trajectory analysis, J. Mol. Model. 7 (2001) 306–317.
[52] E.J. Sorin, V.S. Pande, Exploring the helix-coil transition via all-atom equilibrium ensemble simulations, Biophys. J. 88 (2005) 2472–2493.
[53] S. Pronk, S. Pall, R. Schulz, P. Larsson, P. Bjelkmar, R. Apostolov, M.R. Shirts, J.C. Smith, P.M. Kasson, D. van der Spoel, B. Hess, E. Lindahl, GROMACS 4.5: a high-throughput and highly parallel open source molecular simulation toolkit, Bioinformatics 29 (2013) 845–854.
[54] G.M. Morris, R. Huey, W. Lindstrom, M.F. Sanner, R.K. Belew, D.S. Goodsell, A.J. Olson, AutoDock4 and AutoDockTools4: automated docking with selective receptor flexibility, J. Comp. Chem. 30 (2009) 2785–2791.
[55] G.E. Crooks, G. Hon, J.M. Chandonia, S.E. Brenner, WebLogo: a sequence logo generator, Genome Res. 14 (2004) 1188–1190.